Li and Wang *EURASIP Journal on Wireless Communications and Networking* (2017) 2017:210
DOI 10.1186/s13638-017-0988-y

EURASIP Journal on Wireless Communications and Networking

RESEARCH

Open Access

Sparse representation-based DOA estimation of coherent wideband LFM signals in FRFT domain

Bo Li and Xiuhong Wang*

Abstract

In this paper, the method of direction-of-arrival (DOA) estimation for wideband signals based on sparse representation of FRFT domain is proposed by using the excellent convergence of FRFT to LFM signals. This method focuses the wideband signal to the reference frequency using FRFT, establishes the DOA estimation model and the array manifold matrix in the FRFT domain, and reconstructs the spatial spectral function based on the sparse representation of the spatial angles, so as to realize the wideband LFM signal DOA estimations. The method not only is suitable for non-coherent signals but also can process coherent signals directly without any decoherent operations; in addition, the number of signals is not necessarily known a priori. Simulation results show that the proposed method can achieve better estimation performance and higher angular resolution, especially under low signal-to-noise ratio (SNR) condition.

Keywords: FRFT, DOA, Wideband LFM signal, Sparse representation

1 Introduction

Array signal processing has been widely used in many fields as the main means of spatial domain processing. Because of its large time-bandwidth product, the wideband signal has more abundant information than the narrowband signal. It has been widely used in radar, communication, medicine, seismic exploration, and other fields.

Classical wideband direction-of-arrival (DOA) estimation methods include incoherent signal subspace method (ISSM) [1] and coherent signal subspace method (CSSM) [2–5]. These two methods are based on the frequency domain model of wideband signals and decompose the wideband signals into many narrowband signals with a filter bank or the discrete Fourier transform (DFT). The ISSM method uses only the frequency information of each sub-band in the estimation without taking full advantage of the entire information of the whole band, so its resolution is low and the coherent signals cannot be estimated. The CSSM method transforms the wideband signal to a certain reference frequency through the focusing transformation, thus, all the frequency information of the wideband signal can be effectively synthesized, and then averaging the covariance matrix after focusing, thereby reducing the correlation between the signals, so that the rank of covariance matrix is equal to the number of sources, and the purpose of decoherence is achieved. Finally, the DOA estimation method of narrowband signals is used to estimate the angles. The CSSM method has good estimation accuracy, and the computational complexity is relatively low, but it needs a lot of snapshots as a prerequisite; at the same time, most of the focusing matrices of these algorithms need to pre-estimate the DOA angles, and the focusing matrix is sensitive to the pre-estimated DOA values, especially when the estimated error is large, the overall estimation performance of the algorithm is not ideal.

With the development of sparse representation (SR) theory, sparse representation has also been gradually applied to DOA estimation of wideband signals. The simplest way is to use the ISSM thought, such as Malioutov [6] independently reconstructs the spatial spectrum of each sub-band data and obtain the final sparse solution by averaging. But the independent reconstruction of each sub-band may produce a large difference in the peak position and amplitude of the spatial spectrum of the different sub-bands. Another kind of sparse

* Correspondence: xiuhongwang@hit.edu.cn
School of Information and Electrical Engineering, Harbin Institute of Technology (Weihai), Weihai, China

representation of wideband DOA estimation method is to use CSSM thought, in which the wideband signal is transformed into a narrowband signal by focusing, and then the sparse reconstruction algorithm is used to solve the solution. Zhao [7] used the RSS focusing matrix to focus the wideband signal, and then use the L1-SVD reconstruction algorithm to solve the DOA estimation, while Pan [8] makes the focused array covariance vector to be sparse and solves the sparse resolution by sparse Bayesian learning (SBL). These methods still have the drawbacks of the CSSM method, which requires the angle pre-estimation and be sensitive to the pre-estimation results.

LFM signal is a kind of classical non-stationary signal, which is widely used in radar, sonar, seismic detection, and so on. However, the traditional high-resolution DOA estimation algorithm does not apply to such non-stationary signals; the time-frequency analysis tools are introduced to solve this problem. Fractional Fourier Transform (FRFT) [9–16] is a new time-frequency analysis tool which can reflect the characteristic information of the signal in the time and frequency domain simultaneously. It has excellent aggregation characteristic to the LFM signals but does not have cross-item interference. In FRFT, there is no point selection problem of secondary time-frequency distribution [17]. LFM signals can be easily separated, and their parameters also can be estimated. Therefore, it will obtain better performance than other time-frequency analysis methods by combining FRFT transform and array signal processing to achieve DOA estimation of the wideband LFM signals. It does not have cross-interference, and has excellent focus to the LFM signals. It makes the signal in the FRFT domain concentrated at one point, there is no secondary time-frequency distribution [17] of the point selection problem, making it easy to separate the LFM signal and to be able to estimate the parameters of the LFM simultaneously. Therefore, the combination of FRFT transform and array signal processing to achieve the wideband LFM signal DOA estimation, can achieve better performance than other time-frequency analysis methods.

Therefore, this paper proposes a DOA estimation method of wideband signal based on sparse representation of FRFT domain. The proposed method can deal with coherent signals directly without decoherence processing and avoid the cross-items. It does not need to pre-estimate the angles; at the same time, the number of signals does not need to know. Simulation results show that the proposed method can achieve better estimation performance and higher angular resolution, especially at low SNR.

The rest of this paper is organized as follows: firstly, signal models of wideband LFM signal in the time domain and FRFT domain are introduced in Section 2. Secondly, a DOA estimation method based on sparse model in FRFT domain is proposed in Section 3. Thirdly, the simulation results and some discussions are given in Section 4. Finally, the conclusions of our work are summarized in Section 5.

2 Signal model

2.1 Wideband LFM signal model in time domain

Assuming that the receiving array is a uniform linear array (ULA) with array elements M, the array spacing is d, the number of far field wideband signals $s_k(t)$ $(k = 1, 2, \cdots, K)$ is K, and the direction angles are $(\theta_1, \theta_2, \cdots, \theta_K)$, respectively, the expression of the k^{th} LFM signal is

$$s_k(t) = C_k \exp\left[j\pi\left(2f_k t + \mu_k t^2\right)\right], |t| \leq \frac{T}{2} \tag{1}$$

where C_k, f_k, μ_k, and T represent the amplitude, center frequency, frequency slope, and pulse width of the k^{th} signal, respectively.

The signal received on the m^{th} array element can be expressed as

$$r_m(t) = \sum_{k=1}^{K} s_k(t-\tau_{mk}) + n_m(t) \tag{2}$$

where τ_{mk} represents the delay of the reference signal received by the m^{th} element, which can be expressed as $\tau_{mk} = (m-1)d\sin(\theta_k)/c$ for ULA and c is the speed of light, $n_m(t)$ is the received noise. The LFM signal expression is substituted into Eq. (2), and the received signal can be further expressed as

$$r_m(t) \triangleq \sum_{k=1}^{K} a_m(\theta_k, t) s_k(t) + n_m(t) \tag{3}$$

In Eq. (3), $a_m(\theta_k, t)$ represents the component of the array steering vector on the m^{th} array element, which is defined as

$$a_m(\theta_k, t) = \exp\left[-j2\pi\left(f_k + \mu_k t\right)\tau_{mk} + j\pi\mu_k\tau_{mk}^2\right], m = 1, 2, \cdots, M \tag{4}$$

Integrate all arrays of received signals together, Eq. (4) can be written in matrix form, there are

$$\boldsymbol{r}(t) = \boldsymbol{A}(t)\boldsymbol{s}(t) + \boldsymbol{n}(t) \tag{5}$$

where $\boldsymbol{r}(t) = [r_i(t), r_2(t), \cdots, r_M(t)]^T$ represents the signal vector received by all elements at time t, $\boldsymbol{s}(t) = [s_1(t), s_2(t), \cdots, s_K(t)]$ represents the data vector received by all elements at time t, $\boldsymbol{n}(t) = [n_1, (t), n_2(t), \cdots, n_M(t)]^T$ represents the noise vector received by all elements at time t, $\boldsymbol{A}(t) = [\boldsymbol{a}_1(t), \boldsymbol{a}_2, (t), \cdots, \boldsymbol{a}_K(t)]_{M\times K}$ is the array manifold matrix, and $\boldsymbol{a}_k(t)$ is the steering vector of the k^{th} wideband LFM signal incident on the array which can be expressed as

$$\boldsymbol{a}_k(t) = \begin{bmatrix} a_1(\theta_k, t) \\ a_2(\theta_k, t) \\ \vdots \\ a_M(\theta_k, t) \end{bmatrix} = \begin{bmatrix} \exp\{-j2\pi(f_k + \mu_k t)\tau_{1k} + j\pi\mu_k\tau_{1k}^2\} \\ \exp\{-j2\pi(f_k + \mu_k t)\tau_{2k} + j\pi\mu_k\tau_{2k}^2\} \\ \vdots \\ \exp\{-j2\pi(f_k + \mu_k t)\tau_{Mk} + j\pi\mu_k\tau_{Mk}^2\} \end{bmatrix}, \quad k = 1, 2, \cdots, K \tag{6}$$

It can be seen from the Eq. (6) that the array steering vector changes with time, which makes the traditional DOA estimation method cannot be applied to the direction estimation of the wideband LFM signal, because these methods are based on the fact that the array-oriented vector is a stationary non-time-varying assumption.

2.2 Wideband LFM signal model in FRFT domain

According to the nature of FRFT [9], the LFM signal will have good energy aggregation after a certain order of FRFT transform, that is to say, FRFT transform can bring the energy of LFM signal together, which is similar to "focus" thought. Therefore, we consider converting the received signal to the FRFT field for processing.

The FRFT transform is applied to the signal received on the m^{th} element

$$R_m(u,\alpha) = \boldsymbol{F}^p[r_m(t)] \triangleq \sum_{k=1}^{K} Z_m^k(u,\alpha) + N_m(u,\alpha) \tag{7}$$

where $Z_m^k(u,\alpha)$ is the FRFT transform of the signal $s_k(t - \tau_{mk})$ and $N_m(u,\alpha)$ is the FRFT transform of the noise $n_m(t)$. According to the time shift of the FRFT transform [10], we can get

$$Z_m^k(u,\alpha) = S^k(u-\tau_{mk}\cos\alpha,\alpha)\cdot\exp\left(j\pi\tau_{mk}^2\sin\alpha\cos\alpha - j2\pi u\tau_{mk}\sin\alpha\right) \tag{8}$$

In Eq. (8), $S^k(u,\alpha)$ is the FRFT transform of the signal $s_k(t)$, then

$$S^k(u,\alpha) = \sqrt{\frac{1-j\cot\alpha}{2\pi}}\exp\left(j\pi u^2\cot\alpha\right) \cdot\int_{-T/2}^{T/2}\exp\left[j\pi t^2(\cot\alpha + \mu_k) - j2\pi t(u\csc\alpha - f_k)\right]dt \tag{9}$$

Substituting Eq. (9) into Eq. (8) can get

$$Z_m^k(u,\alpha) = \sqrt{\frac{1-j\cot\alpha}{2\pi}}\cdot\exp\left(j\pi\tau_{mk}^2\sin\alpha\cos\alpha - j2\pi u\tau_{mk}\sin\alpha\right) \cdot\exp\left(j\pi(u-\tau_{mk}\cos\alpha)^2\cot\alpha\right) \cdot\int_{-T/2}^{T/2}\exp\left[j\pi t^2(\cot\alpha+\mu_k) - j2\pi t\left((u-\tau_{mk}\cos\alpha)\csc\alpha - f_k\right)\right]dt \tag{10}$$

It can be seen from the Eq. (10) that the clustering property of the function $Z_m^k(u,\alpha)$ is the best when $\alpha = -\text{arc}\cot(\mu_k) \triangleq \hat{\alpha}_k$, then Eq. (10) can be further reduced to

$$Z_m^k(u,\hat{\alpha}_k) = \sqrt{\frac{1-j\cot\hat{\alpha}_k}{2\pi}}\cdot T\,\frac{\sin[\pi((u-\tau_{mk}\cos\hat{\alpha}_k)\csc\hat{\alpha}_k - f_0)T]}{[\pi((u-\tau_{mk}\cos\hat{\alpha}_k)\csc\hat{\alpha}_k - f_0)T]}\cdot \exp\left(j\pi(u-\tau_{mk}\cos\hat{\alpha}_k)^2\cot\hat{\alpha}_k\right) \cdot\exp\left(j\pi\tau_{mk}^2\sin\hat{\alpha}_k\cos\hat{\alpha}_k - j2\pi u\tau_{mk}\sin\hat{\alpha}_k\right) \tag{11}$$

It can be seen that $Z_m^k(u,\hat{\alpha}_k)$ is a one-dimensional function of u, and when the condition $\hat{u}_k = \tau_{mk}\cos\hat{\alpha}_k + f_0/\csc\hat{\alpha}_k$ is satisfied, the maximum value can be expressed as

$$Z_m^k(\hat{u}_k,\hat{\alpha}_k) = T\sqrt{\frac{1-j\cot\hat{\alpha}_k}{2\pi}}\cdot\exp\left(j\pi(f_0/\csc\hat{\alpha}_k)^2\cot\hat{\alpha}_k\right) \cdot\exp\left(j\pi\tau_{mk}^2\sin\hat{\alpha}_k\cos\hat{\alpha}_k - j2\pi\hat{u}_k\tau_{mk}\sin\hat{\alpha}_k\right) \tag{12}$$

For the reference element, that is, when $m = 1$, the delay $\tau_{mk} = 0$, so Eq. (12) can be expressed as

$$Z_1^k(u,\alpha) = \boldsymbol{F}^p[s_k(t)] = S^k(u,\alpha) \tag{13}$$

The peak size of the function can be expressed as

$$Z_1^k(\hat{u}_{1,k},\hat{\alpha}_{1,k}) = S^k(\hat{u}_{1,k},\hat{\alpha}_{1,k}) = T\sqrt{\frac{1-j\cot\hat{\alpha}_{1,k}}{2\pi}}\exp\left(j\pi\hat{u}_{1,k}^2\cot\hat{\alpha}_{1,k}\right) \tag{14}$$

Where the peak position coordinate is the peak at $(\hat{\alpha}_{1,k},\hat{u}_{1,k})$, $(\hat{\alpha}_{1,k},\hat{u}_{1,k})$ can be expressed as

$$\begin{aligned} \hat{\alpha}_{1,k} &= -\operatorname{arc}\cot\left(\mu_k\right) \\ \hat{u}_{1,k} &= f_0 / \csc\hat{\alpha}_k \end{aligned} \tag{15}$$

The Eq. (12) is further simplified by the Eq. (14) to

$$\begin{aligned} Z_m^k(\hat{u}_k, \hat{\alpha}_k) = S^k(\hat{u}_{1,k}, \hat{\alpha}_{1,k}) \\ \cdot \exp\left(-j2\pi\hat{u}_{1,k}\tau_{mk}\sin\hat{\alpha}_{1,k}\right) \\ \cdot \exp\left(j\pi\tau_{mk}^2\sin\hat{\alpha}_{1,k}\cos\hat{\alpha}_{1,k}\right) \end{aligned} \tag{16}$$

In Eq. (16), since the delay τ_{mk}^2 is small, the exp $\left(j\pi\tau_{mk}^2\sin\hat{\alpha}_{1,k}\cos\hat{\alpha}_{1,k}\right)$ term can be ignored. Thus, Eq. (16) can be further simplified as

$$\begin{aligned} Z_m^k(\hat{u}_k, \hat{\alpha}_k) = S^k(\hat{u}_{1,k}, \hat{\alpha}_{1,k}) \\ \cdot \exp\left(-j2\pi\hat{u}_{1,k}\tau_{mk}\sin\hat{\alpha}_{1,k}\right) \end{aligned} \tag{17}$$

Substituting Eq. (17) into Eq. (7), we can obtain

$$\begin{aligned} R_m(\hat{u}_k, \hat{\alpha}_k) = \sum_{k=1}^{K} S^k(\hat{u}_{1,k}, \hat{\alpha}_{1,k}) \\ \cdot \exp\left(-j2\pi\hat{u}_{1,k}\tau_{mk}\sin\hat{\alpha}_{1,k}\right) \\ + N_m(\hat{u}_k, \hat{\alpha}_k) \end{aligned} \tag{18}$$

where $R_m(\hat{u}_k, \hat{\alpha}_k)$ is a certain peak of the FRFT transform of the received signal of the m^{th} matrix. Summarizing all the elements to receive signals and write them in matrix form, then

$$\boldsymbol{R}(\hat{u}_k, \hat{\alpha}_k) = \boldsymbol{B}(\theta)\boldsymbol{S}(\hat{u}_{1,k}, \hat{\alpha}_{1,k}) + \boldsymbol{N}(\hat{u}_k, \hat{\alpha}_k) \tag{19}$$

where $\mathbf{R}(\hat{u}_k, \hat{\alpha}_k)$ and $\boldsymbol{N}(\hat{u}_k, \hat{\alpha}_k)$ are the corresponding peak-value vector of the received signal vector and the noise vector after FRFT transform. $\boldsymbol{B}(\theta) = [\boldsymbol{b}(\theta_1), \boldsymbol{b}(\theta_2), \cdots, \boldsymbol{b}(\theta_K)]$ is the array manifold matrix of the FRFT domain, where $\boldsymbol{b}(\theta_k)$ is the steering vector in FRFT domain of the k^{th} LFM signal that is incident on the array, and the expression is

$$b(\theta_k) = \begin{bmatrix} \exp\left(-j2\pi\tau_{1k}\hat{u}_{1,k}\sin\hat{\alpha}_{1,k}\right) \\ \exp\left(-j2\pi\tau_{2k}\hat{u}_{1,k}\sin\hat{\alpha}_{1,k}\right) \\ \vdots \\ \exp\left(-j2\pi\tau_{Mk}\hat{u}_{1,k}\sin\hat{\alpha}_{1,k}\right) \end{bmatrix} \tag{20}$$

For ULA arrays, $\tau_{mk} = (m-1)d\sin(\theta_k)/c$. It can be seen from the Eq. (20) that the steering vector of the FRFT domain does not change with time, unlike the steering vector in the time domain of Eq. (6). Therefore, the traditional narrowband DOA estimation methods are applicable to the DOA estimation model in the FRFT domain derived from the Eq. (19). That is to say, we focus the wideband LFM signals through the FRFT transform, thus transforming the wideband DOA estimation model into a DOA estimation model similar to narrowband signals.

3 DOA estimation based on sparse model in FRFT domain

In combination with the above analysis, we reduce the DOA estimation model of the FRFT domain of Eq. (19) to obtain a sparse representation model in the FRFT domain. Firstly, the whole space angle is evenly divided into L parts ($L \gg K$), and the angle set $\boldsymbol{\Theta} \triangleq \left\{\overline{\theta}_1, , \overline{\theta}_2, \cdots, , \overline{\theta}_L\right\}$ is obtained. According to the Eq. (20), a redundant dictionary composed of an over-complete steering vector of the corresponding angle $\boldsymbol{\Theta}$ can be generated

$$\boldsymbol{\Psi}(\boldsymbol{\Theta}) = \left\{\boldsymbol{b}\left(\overline{\theta}_1\right), \boldsymbol{b}\left(\overline{\theta}_2\right), \cdots, \boldsymbol{b}\left(\overline{\theta}_L\right)\right\} \tag{21}$$

The sparse vector $\boldsymbol{H} \triangleq \{h_1, h_2, \cdots, h_L\}$ is defined as the signal amplitude value corresponding to all potential directions $\boldsymbol{\Theta}$. When there is a signal in the presence of $\overline{\theta}_i$, the element h_i is not zero, and its size is exactly the size of the corresponding peak after the FRFT transformation. When there is no incident signal in the potential direction, the element h_i is 0, that is

$$h_i = \begin{cases} S^k\left(\hat{u}_{1,k}, \hat{\alpha}_{1,k}\right), & \overline{\theta}_i \in \{\theta_1, \theta_2, \cdots, \theta_K\} \\ 0, & \overline{\theta}_i \notin \{\theta_1, \theta_2, \cdots, \theta_K\} \end{cases} \tag{22}$$

Therefore, the FRFT domain DOA estimation model of Eq. (19) can be sparse as

$$\boldsymbol{R} = \boldsymbol{\Psi}(\boldsymbol{\Theta})\boldsymbol{H} + \boldsymbol{N} \tag{23}$$

Equation (23) is a sparse representation of all the elements, in which $\boldsymbol{R}$ is the peak value vector obtained from the FRFT transformation of the received signal on all the elements; $\boldsymbol{N}$ is the noise vector of the corresponding peak after FRFT transformed.

In this way, the DOA estimation problem becomes a solution to the sparse representation of Eq. (23). For the solution of this problem, if the minimum l_p norm $(0 < p < 1)$ is used, the sparse solution of the maximum a posteriori (MAP) criterion can be expressed as

$$\begin{aligned} \hat{\boldsymbol{H}}_{\mathrm{MAP}} &= \arg\min_{\boldsymbol{H}} J_p(\boldsymbol{H}) \\ &= \arg\min_{\boldsymbol{H}} \|\boldsymbol{R} - \boldsymbol{\Psi}(\boldsymbol{\Theta})\boldsymbol{H}\|_2^2 + \eta\|\boldsymbol{H}\|_p \end{aligned} \tag{24}$$

where $J_p(\boldsymbol{H}) = \|\boldsymbol{R} - \boldsymbol{\Psi}(\boldsymbol{\Theta})\boldsymbol{H}\|_2^2 + \eta\|\boldsymbol{H}\|_p$ is the cost function, $\eta = \sigma^2/\beta^p$, $\beta = \sqrt{\frac{1}{2^{(2/p)}}\frac{\Gamma(1/p)}{\Gamma(3/p)}}$. The l_p norm is defined as $\|\boldsymbol{H}\|_p = \sum_{i=1}^{L}|\boldsymbol{H}(i)|^p$, $(0 < p < 1)$.

In order to obtain the optimal solution of Eq. (24), we need to satisfy the necessary condition that its derivative is zero

$$\frac{\partial J_p(\boldsymbol{H})}{\partial \boldsymbol{H}} = 2\boldsymbol{\Psi}^{\mathrm{H}}(\boldsymbol{\Theta})\boldsymbol{\Psi}(\boldsymbol{\Theta})\boldsymbol{H}_* - 2\boldsymbol{\Psi}^{\mathrm{H}}(\boldsymbol{\Theta})\boldsymbol{R} + 2\lambda\boldsymbol{\Sigma}\boldsymbol{H}_* = 0 \tag{25}$$

where $\lambda = |p|\eta/2 = |p|\sigma^2/2\beta^p$, $\boldsymbol{\Sigma} = \mathrm{diag}\{|\boldsymbol{H}(1)|^{p-2}, \cdots, |\boldsymbol{H}(L)|^{p-2}\}$. From Eq. (25)

$$\left(\boldsymbol{\Psi}^{\mathrm{H}}(\boldsymbol{\Theta})\boldsymbol{\Psi}(\boldsymbol{\Theta}) + \lambda\boldsymbol{\Sigma}\right)\boldsymbol{H}_* = \boldsymbol{\Psi}^{\mathrm{H}}(\boldsymbol{\Theta})\boldsymbol{R} \tag{26}$$

The weighted minimum iterative solution of FOCUSS is used here to introduce weighted matrices

$$\boldsymbol{W} = \boldsymbol{\Sigma}^{-\frac{1}{2}} = diag\left\{|\boldsymbol{H}(1)|^{1-(p/2)}, |\boldsymbol{H}(2)|^{1-(p/2)}), \cdots, |\boldsymbol{H}(L)|^{1-(p/2)}\right\} \tag{27}$$

then

$$\left[(\boldsymbol{\Psi}(\boldsymbol{\Theta})\boldsymbol{W})^{\mathrm{H}}\boldsymbol{\Psi}(\boldsymbol{\Theta})\boldsymbol{W} + \lambda\boldsymbol{I}\right]\boldsymbol{W}^{-1}\boldsymbol{H}_* = (\boldsymbol{\Psi}(\boldsymbol{\Theta})\boldsymbol{W})^{\mathrm{H}}\boldsymbol{R} \tag{28}$$

Therefore, the optimal solution $\boldsymbol{H}_*$ can be expressed as

$$\boldsymbol{H}_* = \boldsymbol{W}\left[(\boldsymbol{\Psi}(\boldsymbol{\Theta})\boldsymbol{W})^{\mathrm{H}}\boldsymbol{\Psi}(\boldsymbol{\Theta})\boldsymbol{W} + \lambda\boldsymbol{I}\right]^{-1}\cdot(\boldsymbol{\Psi}(\boldsymbol{\Theta})\boldsymbol{W})^{\mathrm{H}}\boldsymbol{R} \tag{29}$$

When the solution of Eq. (29) is changed into FOCUSS iterative process, the iterative relation of the optimal solution $\mathbf{H}_*$ is

$$\begin{aligned}\hat{\boldsymbol{H}}_{k+1} &= \boldsymbol{W}_{k+1}\left(\boldsymbol{U}_{k+1}^{\mathrm{H}}\boldsymbol{U}_{k+1} + \lambda\boldsymbol{I}\right)^{-1}\boldsymbol{U}_{k+1}^{\mathrm{H}}\boldsymbol{R} \\ &= \boldsymbol{W}_{k+1}\boldsymbol{U}_{k+1}^{\mathrm{H}}\left(\boldsymbol{U}_{k+1}\boldsymbol{U}_{k+1}^{\mathrm{H}} + \lambda\boldsymbol{I}\right)^{-1}\boldsymbol{R}\end{aligned} \tag{30}$$

where

$$\boldsymbol{W}_{k+1} = diag\left\{\left|\hat{\boldsymbol{H}}_k(1)\right|^{1-(p/2)}, \cdots, \left|\hat{\boldsymbol{H}}_k(L)\right|^{1-(p/2)}\right\} \tag{31}$$

$$\boldsymbol{U}_{k+1} = \boldsymbol{\Psi}(\boldsymbol{\Theta})\boldsymbol{W}_k \tag{32}$$

In the iterative process, the initial solution can be obtained by the least square solution of Eq. (23)

$$\hat{\boldsymbol{H}}_0 = \boldsymbol{\Psi}^{\mathrm{H}}(\boldsymbol{\Theta})\left[\boldsymbol{\Psi}(\boldsymbol{\Theta})\boldsymbol{\Psi}^{\mathrm{H}}(\boldsymbol{\Theta})\right]^{-1}\boldsymbol{R} \tag{33}$$

The termination condition of the iterative process is the convergence of the optimal solution.

$$\left\|\hat{\boldsymbol{H}}_{k+1} - \hat{\boldsymbol{H}}_k\right\|_2 / \left\|\hat{\boldsymbol{H}}_k\right\|_2 \le \delta \tag{34}$$

where δ is the allowable error. The normalized spatial spectrum is calculated by the sparse solution $\hat{\boldsymbol{H}} = \hat{\boldsymbol{H}}_k$ obtained by iterative convergence.

$$\boldsymbol{P}(\theta) = \frac{|\hat{\boldsymbol{H}}|}{\max\{|\hat{\boldsymbol{H}}|\}} \tag{35}$$

Thus, the angle of DOA estimation of wideband LFM signals can be expressed as

$$\hat{\theta} = \arg\max_{\theta} \boldsymbol{P}(\theta) \tag{36}$$

In summary, the FDSM-ReFOCUSS method is summarized as follows:

1. The FRFT is performed on the received signal $r_0(t)$ of the reference element and the two-dimensional search is performed to extract the peak and the position coordinates $\{(\hat{u}_i, \hat{\alpha}_i)\}i = 1Q$ corresponding to the peak (suppose there are Q peaks and $Q \le K$). The estimated value $\{(\hat{f}_i, \hat{\mu}_i)\}i = 1Q$ of the center frequency and the slope of the Q LFM signal is calculated by the Eq. (15).
2. The fractional Fourier transform of order $\{\hat{p}_i = 2\hat{\alpha}_i/\pi\}_{i=1}^Q$ is calculated for the received signal $r_m(t)$ of all other elements, and the one-dimensional spectral peak is searched and the peak position $\{\hat{u}_i\}_{i=1}^Q$ and the peak size $\{R_m(\hat{u}_i, , \hat{\alpha}_i)\}_{i=1}^Q$.
3. For the $q(q = 1, 2, \ldots, Q)$ spectral peaks, the FRFT domain single snapshot data R is constructed according to Eq. (23); the redundant steering vector matrix $\boldsymbol{\Psi}(\boldsymbol{\Theta})$ is constructed according to Eq. (21).
4. The proposed algorithm is used to solve the sparse solution, and the normalized spatial spectrum $\boldsymbol{P}(\theta)$ is generated according to Eq. (35).
5. The peak value of DOA estimation of wideband LFM signals is obtained by spectral peak search of $\boldsymbol{P}(\theta)$.
6. If $q < Q$, the step (3) is returned to continue, otherwise end the algorithm.

4 Simulation analysis and discussions

In the simulation, different LFM signals are generated according to Eq. (1), and DOA estimation is carried out

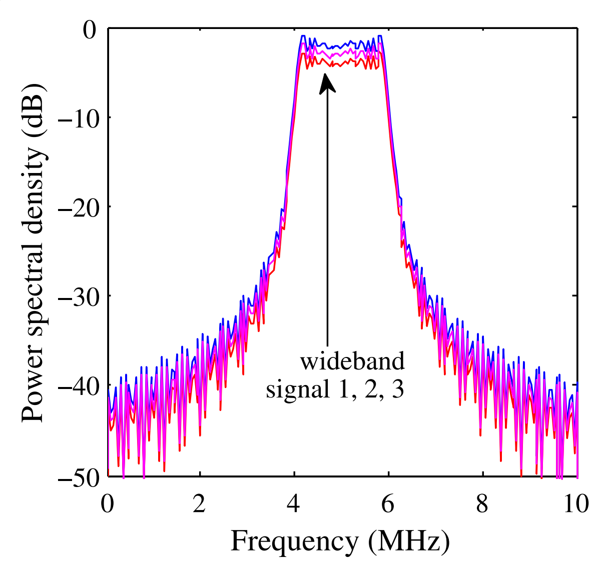

Fig. 1 Energy distribution of coherent LFM signals in the frequency domain

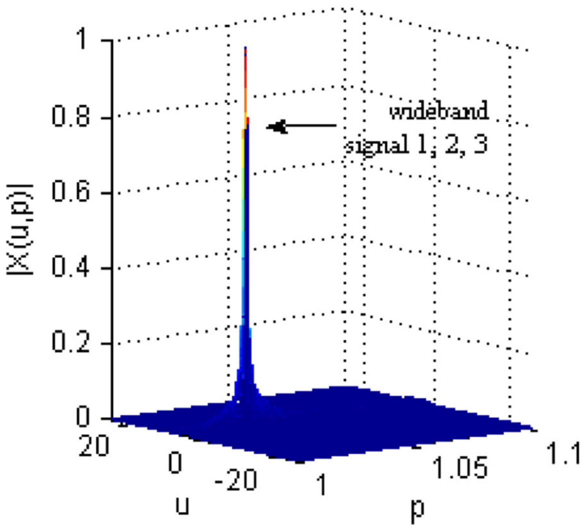

Fig. 2 Energy distribution of coherent LFM signals in the FRFT domain

mainly for the coherent wideband LFM signals, where the coherent LFM signal refers to the center frequency, the frequency modulation slope and the pulse width are the same, but their amplitude may be different. A ULA array with eight elements is used, and the element spacing is the half wavelength of the highest signal frequency.

The simulated SNR is defined as

$$\mathrm{SNR} = 10\lg\left(\frac{1}{K}\sum_{k=1}^{K}\frac{\sigma_{S,k}^2}{\sigma_N^2}\right) \tag{37}$$

where $\sigma_{S,k}^2$ is the power of the k^{th} source, and σ_N^2 is the noise power. The DOA estimation accuracy in the simulation is characterized by the root mean square error (RMSE), which is defined as follows:

$$\mathrm{RMSE} = \sqrt{\frac{1}{KN_c}\sum_{i=1}^{K}\sum_{j=1}^{N_c}\left[\left(\hat{\theta}_{i,j}-\tilde{\theta}_i\right)^2\right]} \tag{38}$$

where K is the number of sources, N_c is the number of independent Monte Carlo trials, $\tilde{\theta}_i$ is the DOA of the i^{th} source, and $\hat{\theta}_i$ is their estimated angle.

The distributions of coherent wideband LFM signals in frequency domain and FRFT domain are compared in Figs. 1 and 2, respectively. There are three coherent wideband LFM signals which have the same center frequency and bandwidth as 5 MHz and 2 MHz, respectively. It can be seen from Figs. 1 and 2, in the case of coherence, the LFM signals cannot be distinguished from each other in the frequency domain or in the FRFT domain. Nonetheless, the LFM signal still has the characteristics of energy aggregation in the FRFT domain, so the wideband LFM signal can be transformed into the FRFT domain for DOA estimation.

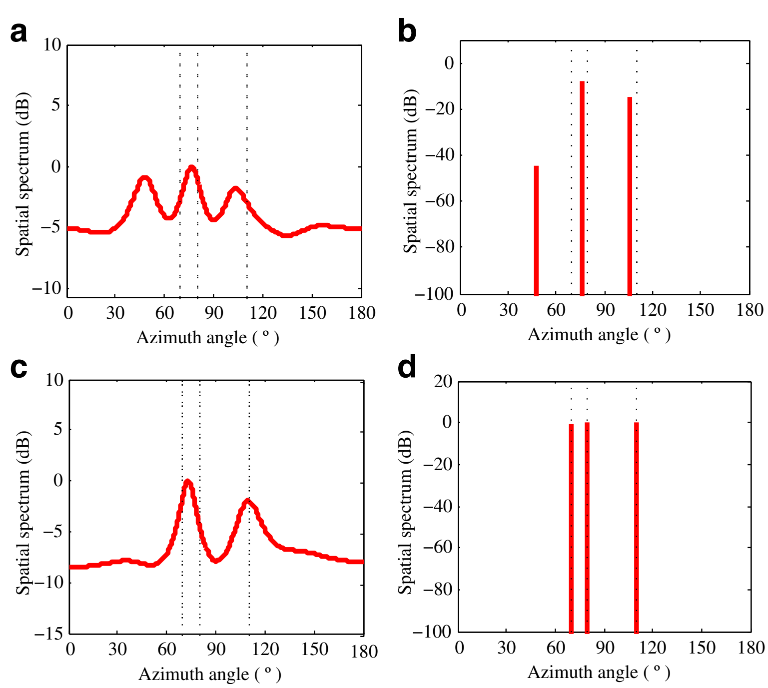

Fig. 3 DOA estimation of different algorithms for coherent wideband LFM signals. **a** RSS-MUSIC algorithm, **b** RSS-L1SVD algorithm, **c** FRFT-SSMUSIC algorithm, and **d** FDSM-ReFOCUSS algorithm

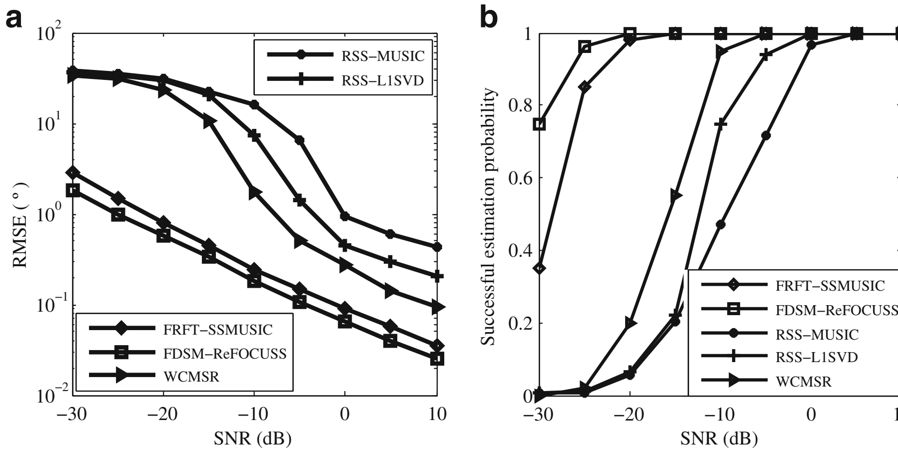

Fig. 4 Estimation performances versus SNR for coherent wideband LFM signals (large angle interval). **a** Estimation error. **b** Successful estimation probability

The spatial spectrums of the different DOA estimation algorithms are compared in Fig. 3. In the simulation, three wideband LFM signals are assumed. The signal parameters of LFM signals are the same as those in Fig. 1; the DOA angles are 71.2°, 80.4°, and 109.5°, respectively. The SNR is − 10 dB. For the RSS-MUSIC algorithm [3] and the RSS-L1SVD algorithm [7] based on RSS focusing transformation, the beamforming (CBF) algorithm [18] is used to pre-estimate the angles.

It can be seen from Fig. 3 that the RSS-MUSIC [3] algorithm, the RSS-L1SVD [7] algorithm, and the FRFT-SSMUSIC [13] algorithm are all invalid. The main reason for the failure of RSS-MUSIC and RSS-L1SVD is that the CBF algorithm has a large error in pre-estimating the angles, due to source angle interval is less than the beam width of the array. In addition, the lower SNR also makes the estimation error larger. Although FRFT-SSMUSIC algorithm can remove the signal coherence using spatial smoothing, its angle resolution is not good. However, the proposed algorithm can estimate the angles of coherent wideband LFM signals very well and has high angular resolution.

Figures 4 and 5 show the DOA estimation performances of different algorithms under different angle intervals. In the simulation, there are two coherent wideband LFM signals, whose center frequency, bandwidth, and pulse width are the same. They are 5 MHz, 2 MHz, and 0.05 s, respectively. The amplitude of the two is different, and the amplitude ratio is 1: 0.8. Figure 4 is a case of the large angle interval, and their angles are 80.1° and 120.3°, respectively, while Fig. 5 is a case of the small angle interval and their angles are 80.1° and 90.5°, respectively.

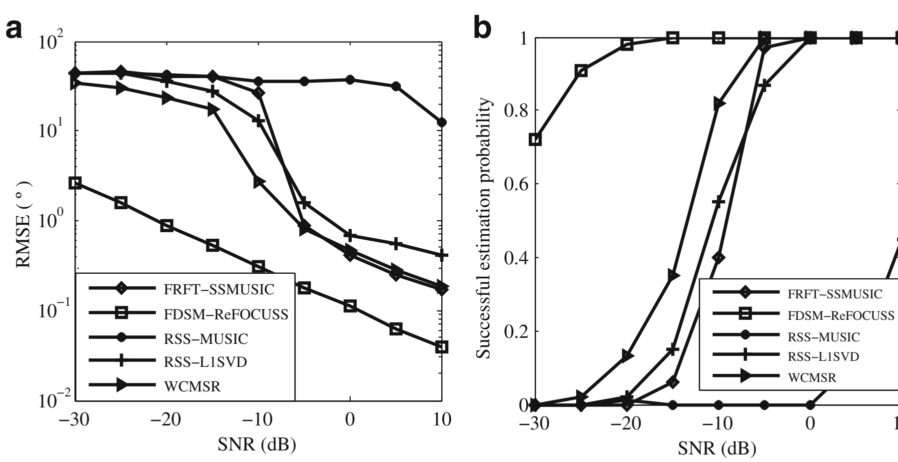

Fig. 5 Estimation performances versus SNR for coherent wideband LFM signals (small angle interval). **a** Estimation error. **b** Successful estimation probability

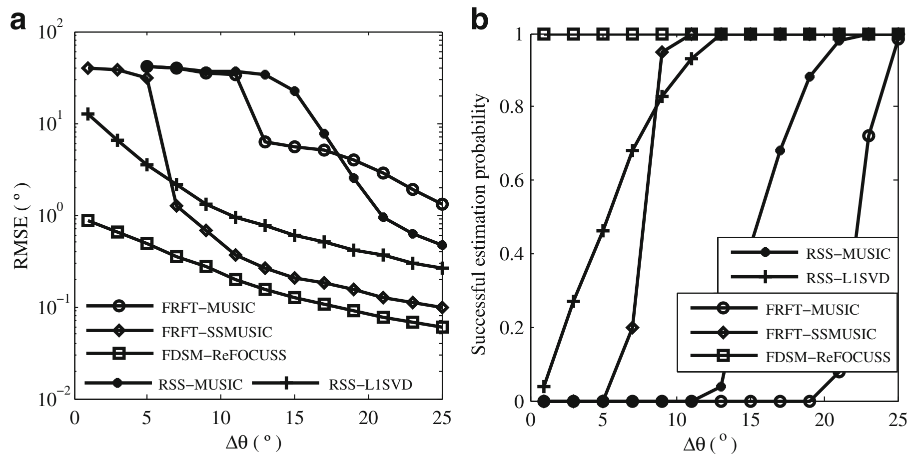

Fig. 6 Estimation performances versus angle difference for coherent wideband LFM signals. **a** Estimation error. **b** Successful estimation probability

It can be seen from Figs. 4 and 5 that the estimation performance of the proposed algorithm is better than other algorithms whether it is large angle interval or small angle interval. Although FRFT-SSMUSIC algorithm has good estimation performance in the case of large angle interval, second only to the proposed algorithm, but in the case of small angle interval, its performance is poor, especially at low SNR. The performance of the WCMSR algorithm is better than RSS-L1SVD and RSS-MUSIC, but these three algorithms have larger estimation error in the low SNR conditions, especially RSS-MUSIC algorithm, which cannot work at low SNR.

Figure 6 shows the relationship between DOA estimation performances and the angle difference of the two signals. For the RSS-MUSIC and RSS-L1SVD algorithms, the ideal DOA pre-estimation is used. The signal parameters of LFM signals are the same as those in Fig. 4 and the SNR is set 0 dB.

It can be seen from Fig. 6 that the estimation performance of the proposed algorithm is better than other algorithms whether in estimation error or in successful estimation probability. However, the performance of FRFT-SSMUSIC algorithm is poor when the angle difference is less than 5°. The RSS-MUSIC algorithm has larger estimation error when the angle difference is less than array beam width (16.4°), whereas when the angle difference is greater than array beam width, its estimation error will decrease with the increase of the angle difference. The RSS-L1SVD algorithm is better than RSS-MUSIC algorithm, although its performance is less than the proposed algorithm.

5 Conclusions

In this paper, the FRFT transform is used to estimate the LFM signals, and a DOA estimation method for wideband LFM signal based on sparse representation is proposed. The proposed method can deal with coherent signals directly without decoherence processing and avoid the cross-item interference. It does not need to pre-estimate the angles; at the same time, the number of signals does not need to know a priori. Simulation results show that the proposed method can achieve better estimation performance and higher angular resolution than the traditional methods, especially under the low SNR and small angle difference conditions.

Acknowledgements

This work is supported in part by the National Natural Science Foundation of China (No. 61401118, No. 61371100, and No. 61671184), the Natural Science Foundation of Shandong Province (No. ZR2014FP016), the Foundation of Science and Technology on Communication Networks Key Laboratory, and the Fundamental Research Funds for the Central Universities (No. HIT.NSRIF.2016100 and 201720).

Funding

The National Natural Science Foundation of China (Grant Nos. 61401118, 61371100, and 61671184) is supporting the data acquisition devices and materials. The Natural Science Foundation of Shandong Province (Grant No. ZR2014FP016) and the Foundation of Science and Technology on Communication Networks Key Laboratory are supporting the simulations; and the Fundamental Research Funds for the Central Universities (Grant Nos. HIT.NSRIF.2016100 and 201720) are supporting the data analyses.

Authors' contributions

BL conceived and designed the experiments; XW performed the experiments; BL and XW wrote the paper. All authors have read and approved the final manuscript.

Competing interests

The authors declare that they have no competing interests.

Publisher's Note

Springer Nature remains neutral with regard to jurisdictional claims in published maps and institutional affiliations.

Received: 28 June 2017 Accepted: 15 November 2017
Published online: 11 December 2017

References

1. M Max, T Shan, T Kailath, Spatio-temporal spectral analysis by eigenstructure methods. IEEE Trans. Acou. Speech & Sig. Proce. **32**(4), 817–827 (1984)
2. H Wang, M Kaveh, Coherent signal-subspace processing for the detection and estimation of angles of arrival of multiple wide-band sources. IEEE Trans. Acou. Speech & Sig. Proce. **33**(4), 823–831 (1985)
3. H Hung, M Kaveh, Focussing matrices for coherent signal-subspace processing. IEEE Trans. on Acou. Speech & Sig. Proce. **36**(8), 1272–1281 (1988)
4. MA Doron, AJ Weiss, On focusing matrices for wide-band array processing. IEEE Trans. Sig. Proce **40**(6), 1295–1302 (1992)
5. S Valaee, P Kabal, Wideband array processing using a two-sided correlation transformation. IEEE Trans. Sig. Proce. **43**(1), 160–172 (1995)
6. D Malioutov, M Cetin, AS Willsky, A sparse signal reconstruction perspective for source location with sensor arrays. IEEE Trans. Sig. Proce **53**(8), 3010–3022 (2005)
7. Y Zhao, L Zhang, et al., A new DOA estimation method for wideband signals based on sparse representation. J. Elec. and Inf. **37**(12), 2935–2940 (2015)
8. Y Pan, H Lu, H Zhu, et al., in *IEEE China Summit and International Conference on Signal and Information Processing*. DOA estimation for coherent and incoherent wideband sources via sparse representation of the focused array covariance vectors (2006)
9. LB Almeida, The fractional fourier transform and time-frequency representations. IEEE Trans. Sig. Proce **42**(11), 3084–3091 (1994)
10. T Ran, *Fractional Fourier Transform and Its Application* (Tsinghua University Press, Beijing, 2009)
11. K Huang, D Tian, T Chen, FrFT-MUSIC algorithm for estimating WLFM signal DOA based on time domain convergence and compensation. Sig. Proce. **19**(1), 44–47 (2003)
12. R Tao, Y Zhou, A new algorithm for wideband LFM signal direction estimation based on fractional Fourier transform. J. Beijing Ins. Tech. **25**(10), 895–899 (2005)
13. H Qu, L Qi, X Mu, et al., in *International Conference on Innovative Computing, Information and Control*. DOA estimation of coherent wideband LFM signals based on fractional Fourier transform (2006), pp. 18–21
14. X Liu, J Wang, M Huang, DOA estimation of wideband LFM coherent signals based on fractional Fourier transform. Data Acqu. Proce. **23**(5), 45–48 (2008)
15. F Ye, Y Li, S Yang, in *International Symposium on Systems and Control in Aerospace and Astronautics*. 2-D DOA estimation of LFM signal based on FRFT (2006), pp. 1080–1083
16. Y Zhang, L Qi, X Mu, et al., in *International Conference on Innovative Computing, Information and Control*. 2-D DOA estimation of wideband LFM signal in fractional Fourier domain (2006), pp. 6–9
17. S Chandran, MK Ibrahim, DOA estimation of wide-band signals based on time-frequency analysis. IEEE J Ocea. Engi. **24**(1), 116–121 (1999)
18. LC Godara, Application of antenna arrays to mobile communications. II. Beamforming and direction-of-arrival considerations. Proc. IEEE **85**(8), 1195–1245 (1997)